Metrol. Meas. Syst., Vol. 26 (2019) No. 4, pp. 687–696
DOI: 10.24425/mms.2019.130568

METROLOGY AND MEASUREMENT SYSTEMS
Index 330930, ISSN 0860-8229
www.metrology.pg.gda.pl

EVALUATION OF THE RESIDUAL MAGNETIC FIELD MEASUREMENT SYSTEM FOR EARLY IDENTIFICATION OF RAILWAY DEFECTS

Mirosław Rucki, Anna Gockiewicz, Tadeusz Szumiata

Kazimierz Pulaski University of Technology and Humanities in Radom, Faculty of Technical Engineering, Malczewskiego 29, 26-600 Radom, Poland (✉ *m.rucki@uthrad.pl*, +48 48 361 7696, *agockiewicz@op.pl*, *t.szumiata@uthrad.pl*)

Abstract

The paper presents research on the capability of the residual magnetic field (RMF) measurement system to be applied to the railway inspection for the early non-destructive detection of defects. The metal magnetic memory (MMM) phenomena are analysed using normal component H_y of self-magnetic flux leakage (SMFL), and its tangential component H_x, as well as their respective gradients. The measurement apparatus is described together with possible factors that may affect the results of measurement. The Type A uncertainty estimation and repeatability tests were performed. The results demonstrate that the system may be successfully applied to detection of head check flaws.

Keywords: residual magnetic field, measurement, rail inspection, uncertainty, repeatability.

1. Introduction

Inner structural defects in the railway tracks have a huge impact on the safety of passengers, especially because of the continual increase of speed and load of trains. Inspection and maintenance efforts should be made in order to minimize probability of failures and derailments caused by *rolling contact fatigue* (RCF) and wear [1]. Thus, a great deal of research is performed in order to develop effective and fast non-destructive methods of early detection of flaws. Among others, an automatic visual detection system was proposed, co that the squad type flaws can be found before a crash takes place. The author reported a detection rate of 94% [2]. Coherence Correlation Interferometry was reported to be applied to detection of head flaws in rails [3]. Other publications proposed a method based on simplified laser scatterometry to detect squats [4], or infrared information combined with visible images [5], but the optical techniques can detect only the visible surface damages. The ultrasonic method, in turn, is ineffective for surface defects and enables to analyse mostly defects under the rail head surface. It was demonstrated that more than 60% of surface defects remain undetected by the ultrasonic method [6].

A method based on eddy currents enables to detect hidden defects inside the material, but it requires keeping a constant distance between the sensor and the surface of the rail, which is difficult in real conditions [7]. Nevertheless, a system based on eddy currents was applied in rail grinders by German Railways (DB) [8]. An interesting study was presented, aiming to evaluate different methods of geometric descriptions of squat crack networks; through X-ray radiography complemented with geometric reconstruction, metallography, X-ray tomography, and topography measurements [9]. However, the lack of effective non-destructive methods for detecting head defects in tracks in service is obvious, so that some authors suggest to apply combinations of several methods [10]. The paper [10] contains an extensive review of the existing methods of rail health monitoring.

Moreover, there are no standards concerning the inner small-size defects detected in rails with MMM methodology. The presented research aiming to evaluate a rail inspection method based on the metal magnetic memory, is the first step towards a complex solution of this problem.

2. Measurement principle

In the research, the passive *non-destructive technique* (NDT) based on the *metal magnetic memory* (MMM) was applied. It consists of registration and analysis of variations of the *residual magnetic field* (RMF) and its gradients on the surface of examined detail [11]. The initial research provided a possibility of quantitative defect identification for ferromagnetic steels, because characteristic parameters of the abnormal magnetic changes were capable of capturing the defect's location and shape [12]. It was demonstrated also that the three-dimensional finite element analysis of the residual magnetic field can be successfully applied to ferromagnetic materials subjected to an early damage [13]. The methodology was found suitable for identification of stress concentration areas, as well as defects due to non-uniformity of the ferromagnetic structure [14], especially under load [15]. Generally, MMM tests can only find the possible locations of defects without quantitative characteristics of the defects, though some theoretical propositions based on a linear magnetic-charge model were reported [16].

The measurement technique utilizes the following physical phenomena. *Self-Magnetic Flux Leakage* (SMFL) signals are generated in the stress-concentration zones of a ferromagnetic material. The residual magnetic field appears around accumulations of high-density dislocations under working loads or around the maximal non-uniformity in the structure [17]. When magnetic metals are strained, they are irreversibly transformed from the non-magnetic state into the magnetic state [14]. Thus, RMF reflects irreversible magnetic changes in the direction of internal stress formation, either in load conditions or as a result of structural changes in the metal.

For the MMM diagnostic of a rail, the basic theoretical assumption is made, that the internal stress σ evokes a local change of the magneto-crystalline anisotropy, which can be described by an effective magnetizing field, *i.e.* effects on the magnetization. Such a magneto-mechanical mechanism is known as the Villari effect or the inverse magnetostrictive phenomenon. According to the models described in [18–20]:

$$\Delta M(\sigma) \approx \frac{9}{2} \frac{M_r}{\mu_0 M_s^2} \lambda_s(\sigma) \cdot \sigma \cdot \mu_r, \tag{1}$$

where:

ΔM – local (stress-induced) change of the magnetization;

σ – effective stress;

$\lambda_s(\sigma) = \lambda_s(0) + k\sigma$ – stress dependent saturation magnetostriction constant [21–22];

Metrol. Meas. Syst., Vol. 26 (2019), No. 4, pp. 687–696
DOI: 10.24425/mms.2019.130568

λ_s (0) – zero-stress saturation magnetostriction constant;
k – coefficient of stress correction to saturation magnetostriction constant;
M_s – saturation magnetization of the material;
M_r – remanent magnetization of the material;
μ_r – relative magnetic permeability of the medium;
μ_0 – magnetic permeability of the vacuum.

This perturbation of the local magnetization produces an additional magnetic field (just around the internal stress region) which can be detected by a magnetometer. The distribution of such a magnetic field can be predicted theoretically by means of magneto-static *finite elements methods* (FEMs).

In the NDT methodology, also the effect of leakage magnetic field scattering in the concentration zone of stress and deformation is important. Moreover, the phenomenon of appearing magnetic domains on the dislocation walls and around the stress concentration zones plays an important role in the measurement.

During the analysis of MMM, two main parameters are employed:

– normal component H_y [A/m] of SMFL, and its tangential component H_x [A/m];
– respective gradients of the abovementioned components $\frac{dH_y}{dx}$ [kA/m^2] and $\frac{dH_x}{dx}$ [kA/m^2] in the examined length x.

In the presented initial stage of research program, components H_y and H_x were considered, because they are measured directly by the apparatus, and thus their distribution characterize the device capability. In the future, the gradients will undergo the thorough statistical analysis, because they are more sensitive to the inner defects, but also more affected by errors of various types.

3. Measurement apparatus

In the experimental research, a piece of rail was taken from a real railway under the jurisdiction of Zakład Linii Kolejowych in Skarżysko-Kamienna (Poland). The examined rail had *head checking* (HC) defects, *i.e.* micro-cracks at the gauge corner of the rail.

The piece of rail was examined by a dedicated microprocessor-controlled ferrometer TSC1M-4 produced by Energodiagnostika company (Russia). This magnetometer is equipped with flux-gate magnetic field detectors (transducers) of longitudinal and transversal DC magnetic field. Their high sensitivity originates from a strong dependence of AC response on DC external magnetic field – owing to specific properties of the soft magnetic core. The principle of defectoscopic method is based on the application of such magnetometers to detection of residual magnetic fields generated by flaws located in the object surface layer. This idea, called metal *magnetic memory method* (MMM), was proposed for the first time by Dubov [23]; a scheme of the dedicated magnetometer is shown in Fig. 1.

An advantage of this method with respect to other AC and DC magnetic methods (like eddy currents, AC susceptibility, DC scattered fields) is the fact that it does not require any external magnetizing. This makes the measurement equipment relatively simple and enables to use small-size detecting heads. Moreover, this method does not change the magnetic state of examined object. All these features enable to detect very fine, subsurface defects at a very early stage of their development. Good examples are so called "head-checking" flaws in railway rails, which are not visible directly on the surface, but constitute regions of the strong stress concentration inside the material. These internal stresses are sources of additional, local magnetization and

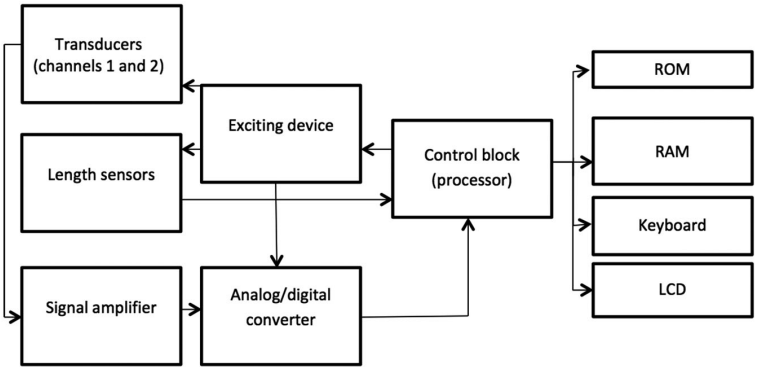

Fig. 1. A scheme of the magnetometer (based on [21]).

the magnetic field evoked by the Villari effect [21, 22], known as the inverse magnetostriction phenomenon. The main serious limitation of MMM method lies in the not obvious relation between the magnetic fields measured around the flaw and the value of the stress (as well as the size of the flaw), so that the application of advanced models is necessary to assess the detected flaws. Moreover, MMM method does not offer detailed magnetic characteristics like full magnetic hysteresis loops' measurements, the Barkausen noise method or *magneto-acoustic emission* (MAE), which are valid for non-zero magnetostrictic materials. These techniques, based on the phenomenon of magnetic domain structure modification by external and internal stress, are widely used *e.g.* for the studies of plastically deformed steel elements [24, 25]. However, in order to perform measurements using the abovementioned techniques, a large-size experimental setup (including a magnetizing coil and a soft magnetic core) is necessary [24], as well as specially prepared specimens of materials. Hence, it is impossible to use this kind of system for the monitoring of fine head checking flaws in rails, while MMM method remains suitable for this purpose, since it is based on detection of residual magneto-static fields with small-size sensors.

The magnetometer enables to evaluate inner stresses and deformations, and to identify areas of stress concentration. Its technical data are as follows: a measurement range $H = \pm 2000$ A/m, magnetic field sensitivity ±1 A/m, two measurement channels, the minimal measurement step 1 mm, the maximal scanning speed 0.2 m/s, a working range of temperature from −20°C to +60°C, a range of specific humidity 45%÷80% without condensation.

The experiments were performed in repeatable conditions, with the same measurement procedure, the same measurement instrument used in the same conditions, the same observer, in the same location, and repetitions were made over a short period [26]. During the measurements, temperature was kept at 21°C ±1°C. The device was placed in a trolley shown in Fig. 2, and moved along the examined piece of rail. The movement was repeated with measurement performed on the part of rail marked by black lines shown in Fig. 2. The interval between those lines was 100 mm, the first line corresponded to coordinate $x = 0$, and the second one – to $x = 100$ mm.

The obvious problem with measurement accuracy in the case of quantitative defect identification is the lack of direct relation between the dimensions of a micro-crack and the measured characteristics of magnetic field. This kind of relation cannot be established with non-destructive methods only, since the real structure of material inside the rail is unknown.

In the case of qualitative characteristics, the measurement systems provide measurement values of the controlled characteristics, which require task-related measurement systems [27].

Metrol. Meas. Syst., Vol. 26 (2019), No. 4, pp. 687–696
DOI: 10.24425/mms.2019.130568

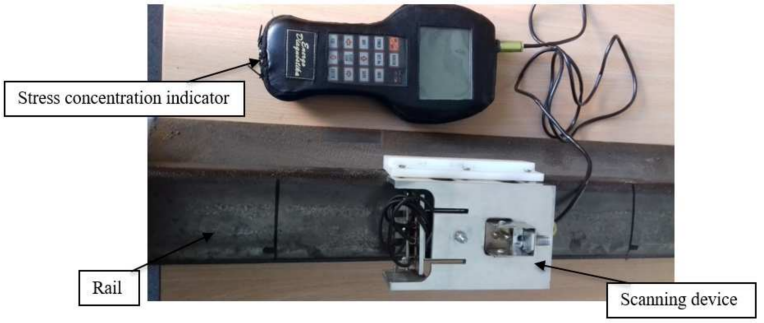

Fig. 2. A photo of the measurement setup.

Thus, in order to evaluate the capability of the system to identify possible defects and inner damages, it was decided to examine its repeatability statistically [26]. An *equipment variation* (EV) parameter was chosen, because it reflects the variation range of the operator's repeated measurements, and is applicable to various systems [28–30].

4. Repeatability test results and discussion

First of all, the expanded uncertainty $U_{0.99}$ for a confidence level $p = 99\%$ was calculated in the case of both components of SMFL: normal component H_y, and tangential component H_x [A/m]. In order to maintain repeatability conditions, especially a short time interval, 10 repetitions were made. In that case, the coverage factor is equal to the Student's distribution quantile $t_{\alpha,n}$. Figs. 3–6 present graphs of values obtained during repetitions. Respective values obtained from the first repetition represent the curves' numbers Hx1 (Fig. 3) and Hy1 (Fig. 4), and each subsequent repetition provided the next numbers – up to Hx10 and Hy10. On the other hand, Figs. 5 and 6 contain graphs of derivatives, for the first repetition dHxdx1 (Fig. 5) and dHydx1 (Fig. 6), and for each subsequent repetition the next numbers were given – up to dHxdx10 and dHydx10, respectively.

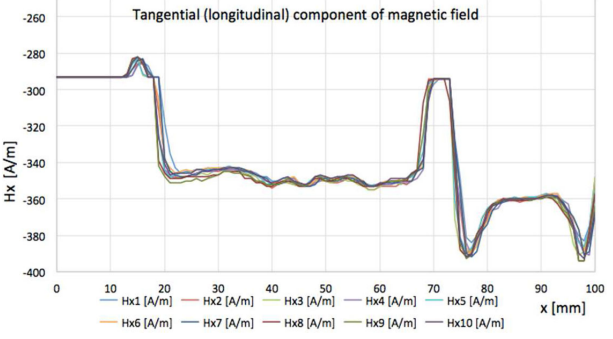

Fig. 3. Graphs of tangential component H_x of magnetic field.

There are two clear extrema of gradients of tangential component H_x distinguishable at $x = 23$ mm and at $x = 77$ mm shown in Fig. 3, and corresponding extrema of gradients of

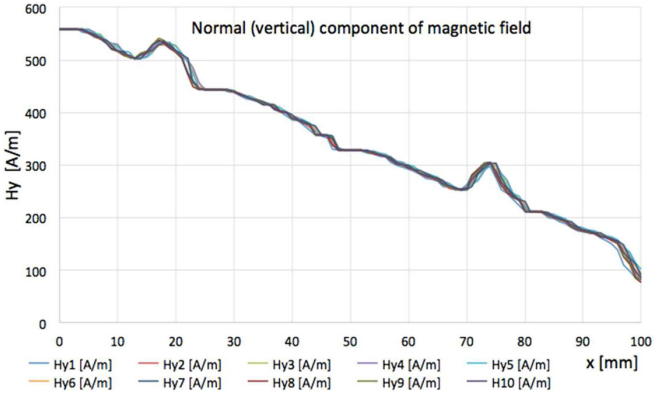

Fig. 4. Graphs of normal component H_y of magnetic field.

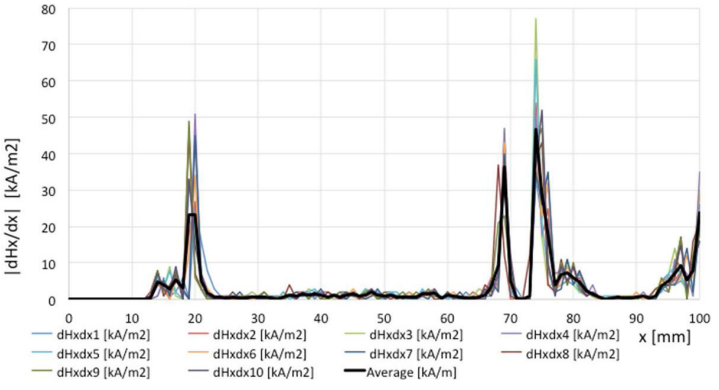

Fig. 5. Graphs of gradients of tangential component dH_x/dx of magnetic field.

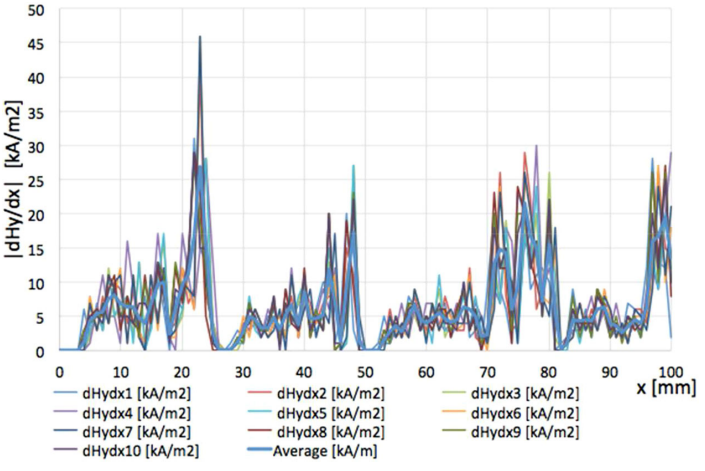

Fig. 6. Graphs of gradients of normal component dH_y/dx of magnetic field.

Metrol. Meas. Syst., Vol. 26 (2019), No. 4, pp. 687–696
DOI: 10.24425/mms.2019.130568

normal component H_y, shifted to $x = 20$ mm and $x = 76$ mm shown in Fig. 4, respectively. The examined device provided magnetic field components with accuracy of 1 A/m, and linear point identification on the rail length was made with resolution 1 mm. Tables 1 and 2 present the respective values obtained during repetitions that became the basis for further estimation of uncertainty, given below each table.

Table 1. Results obtained for 10 repetitions at the point $x = 23$ mm.

No.	1	2	3	4	5	6	7	8	9	10	Average
Hx_{23} [A/m]	−346	−349	−348	−349	−346	−345	−348	−349	−351	−346	−347.7

The standard deviation can be treated as a standard uncertainty u, so it can be written: $\overline{H_x} = 347.7$ A/m, $u(H_x) \approx s_{H_x} = 1.89$ A/m.

Since the measurement was repeated 10 times, to obtain the expanded uncertainty the Student's distribution quantile $t_{\alpha,n}$ was applied. For a confidence level $p = 0.99$ and 10 repetitions, $t_{\alpha,n} = 3.250$. Substituting it as a coverage factor k to the formula:

$$U = k \cdot u, \tag{2}$$

the following was obtained: $U_{0.99} = 3.250 \times u(H_x) = 6.14$ [A/m]. The same was done for the H_x values obtained at the point $x = 77$ mm.

Table 2. Results obtained for 10 repetitions at the point $x = 77$ mm.

No.	1	2	3	4	5	6	7	8	9	10	Average
Hx_{77} [A/m]	−384	−388	−388	−391	−387	−390	−392	−390	−391	−391	−389.2

The average value and standard uncertainty were calculated as follows: $\overline{H_x} = 389.2$ A/m, $u(H_x) \approx s_{H_x} = 2.44$ A/m.

Similarly, for a confidence level $p = 0.99$ and 10 repetitions, $t_{\alpha,n} = 3.250$. Thus, the expanded uncertainty for tangential component H_x at the point $x = 77$ mm can be estimated as follows: $U_{0.99} = 3.250 \times u(H_x) = 7.93$ [A/m].

It should be noted that at the point $x = 23$ mm, the expanded uncertainty $U_{0.99}$ was ±6.14 A/m, which was approximately 1.8% of the measured value of tangential component H_x. However, at the point $x = 77$ mm, the expanded uncertainty $U_{0.99}$ was ca. 23% larger, *i.e.* ±7.93 A/m. That is why it is necessary to estimate also the value of equipment variation EV, which represents the amount of measurement system variation compared with the process variation. In the case of the rail NDT, the system variation can be compared with the variation of measured value along the rail.

According to the procedure [27], the results of 10 repetitions of the H_x measurement at two different points were used for further calculations according to the formula:

$$\sum E = \sum_{i=1}^{n} \sum_{j=1}^{k} (X_{ij} - X_{i\bullet})^2, \tag{3}$$

where:

$X_{i\bullet}$ – average value obtained for a certain point x along the rail;

i – number of points along the rail, from 1 to n; in that case $n = 2$;

j – number of repetitions from 1 to k; in that case $k = 10$.

The results of calculations are presented in Table 3.

Table 3. H_x repeatability calculation results.

No.	1	2	3	4	5	6	7	8	9	10	$X_{i\bullet}$	$\sum_{j=1}^{k}\left(X_{ij}-X_{i\bullet}\right)^2$
Hx_{1j} [A/m]	−346	−349	−348	−349	−346	−345	−348	−349	−351	−346	−347.7	32.1
Hx_{2j} [A/m]	−384	−388	−388	−391	−387	−390	−392	−390	−391	−391	−389.2	53.6
												$\sum E = 85.7$

The obtained results were substituted into the following equations:

$$s_E^2 = \frac{1}{n(k-1)} \sum E \tag{4}$$

and:

$$EV = 5.15\, s_E. \tag{5}$$

This way the value of equipment variation was estimated as $EV = 11.2$ A/m for a confidence level of 99%. This value is very close to the uncertainty interval $\pm U_{0.99}$ calculated for the point $x = 23$ mm, namely, ±6.14 A/m. Since the "process variation" is not known, and various values can be expected along hundred kilometres of rails in real working conditions, the initial value $H_x = 293$ A/m at the point $x = 0$ was assumed as a reference value RF. Then, the Percent Equipment Variation $\%EV$ can be calculated as follows:

$$\%EV = \frac{EV}{RF} \cdot 100\% = 3.8\%. \tag{6}$$

Finally, since the new measurement system is considered to be good for a specific task if it reveals Percent Equipment Variation $\%EV$ below 10%, it was assumed that $\%EV = 3.8\%$ is highly satisfactory.

In the case of normal component H_y, it is difficult to determine a reference value RF, because of steady declination of its value from 600 down to 100 A/m within the measured rail interval of 100 mm. Nevertheless, the equipment variation EV was calculated accordingly from the collected data shown in Table 4.

Table 4. H_y repeatability calculation results.

No.	1	2	3	4	5	6	7	8	9	10	$X_{i\bullet}$	$\sum_{j=1}^{k}\left(X_{ij}-X_{i\bullet}\right)^2$
Hy_{1j} [A/m]	530	530	535	534	534	531	532	537	541	536	−534.0	108.0
Hy_{2j} [A/m]	297	302	300	304	298	303	304	305	306	305	−302.4	86.4
												$\sum E = 194.4$

Thus, the value of equipment variation during normal component H_y measurement was estimated as $EV = 16.9$ A/m for a confidence level of 99%. It is noteworthy, that it is close to the value $EV = 11.2$ A/m estimated for tangential component H_x.

Metrol. Meas. Syst., Vol. 26 (2019), No. 4, pp. 687–696
DOI: 10.24425/mms.2019.130568

5. Conclusions

Analysis of the measurement system based on MMM phenomenon demonstrated that the system can be successfully used for early identification of railway inner defects. Changes in the surface magnetic field correspond to displacements and stress concentration inside the ferromagnetic material. The equipment variation for a confidence level of 99% was calculated for both tangential and normal components of magnetic field, and the obtained values $EV = 11.2$ A/m and $EV = 16.9$ A/m, respectively, were found satisfactory. In the case of tangential component H_x, Percent Equipment Variation was estimated as $\%EV = 3.8\%$. At the present stage of research, a similar estimation for normal component H_y was not possible because of difficulties with the reference value. In the further analysis, it will be necessary to make measurements along a longer interval x, at least several meters if not kilometres, which will be much closer to real conditions of the possible use of the examined device. Also, additional tests must be made in order to determine critical values of the measured magnetic field scattering related to the critical damages and stresses inside the rail material.

Acknowledgement

This work was supported by the University of Technology and Humanities in Radom under statutory grant 3179/25/P-DBUPB/2015/063.

References

[1] Magel, E., Mutton, P., Ekberg, A., Kapoor, A. (2016). Rolling contact fatigue, wear and broken rail derailments. *Wear*, 366–367, 249–257.

[2] Bojarczak, P. (2014). Detection of squat defects in railway. *Welding Technology Review*, 86(10), 12–16.

[3] Lesiak, P., Wlazło, M. (2014). Detection of head checking flaws in railway rails using an optical method. *Scientific works of the Warsaw University of Technology*, 104, 33–42.

[4] Lesiak, P., Szumiata, T., Wlazło, M. (2015). Laser scatterometry for detection of squat defects in railway rails. *The Archives of Transport*, 33(1), 47–56.

[5] Tang, Ch., Tian, G.Y., Chen, X., Wu, J., Li, K., Meng, H. (2017). Infrared and visible images registration with adaptable local-global feature integration for rail inspection. *Infrared Physics & Technology*, 87, 31–39.

[6] Bojarczak, P. (2013). *Visual diagnostics of the rails*. Radom: ITE – PIB Radom.

[7] Hansen, J., Calvert, J. (2002). Eddy current testing. A solution to detecting rolling contact fatigue in rail? *Proc. of 5th international conference and exhibition*, London, UK, 3–4 July.

[8] Meierhofer, R., Pohl, R. (2006). Head Check Measurement – a Fully-operational System on a Rail Grinder. *Proc. of World Congress on Railway Research*, Montreal, Canada, 2006.

[9] Jessop, C., Ahlström, J., Hammar, L., Fæster, S., Danielsen, H.K. (2016). 3D characterization of rolling contact fatigue crack networks. *Wear*, 366–367, 392–400.

[10] Popović, Z., Lazarević, L., Brajović, L., Vilotijević, M. (2015). The Importance of Rail Inspections in the Urban Area – Aspect of Head Checking Rail Defects. *Procedia Engineering*, 117, 596–608.

[11] Roskosz, M., Fryczkowski, K. (2015). Analysis of the possibility of identification of stress state based on residual magnetic field of ferromagnetic material. *Welding Technology Review*, 87(12), 75–77.

[12] Bao, Sh., Fu, M., Lou, H., Bai, Sh. (2017). Defect identification in ferromagnetic steel based on residual magnetic field measurements. *J. Magnetism Magn. Mater.*, 441(1), 590–597.

[13] Yao, K., Shen, K., Wang, Zh.D., Wang, Y.Sh. (2014). Three-dimensional finite element analysis of residual magnetic field for ferromagnets under early damage. *J. Magnetism Magn. Mater.*, 354(1), 112–118.

[14] Wilson, J.W., Tian, G.Y., Barrans, S. (2007). Residual magnetic field sensing for stress measurement. *Sensors and Actuators A: Physical*, 135(2), 381–387.

[15] Gontarz, Sz., Szulim, P., Lei, Y. (2018). Identification of magnetomechanical phenomena in a degradation process of loaded steel elements. *J. Magnetism Magn. Mater.*, 467(1), 29–36.

[16] Wang, Z.D., Yao, K., Deng, B., Ding, K.Q. (2010). Quantitative study of metal magnetic memory signal versus local stress concentration. *NDT & E International*, 43(6), 513–518.

[17] Dubov, A. (2006). Principle features of metal magnetic memory method and inspection tools as compared to known magnetic NDT methods. *CINDE Journal*, 27(3), 16–20.

[18] Zhu, B., Lo C.C.H., Lee, S.J., Jiles, D.C. (2001). Micromagnetic modeling of the effects of stress on magnetic properties. *J. Appl. Phys.*, 89, 7009–7011.

[19] Jiles, D.C., Devine, M.K. (1994). Recent developments in modeling of the stress derivative of magnetization in ferromagnetic materials. *J. Appl. Phys.*, 76(10), 7015–7017.

[20] Szewczyk, R., (2016). Stress-induced anisotropy and stress dependence of saturation magnetostriction in the Jiles–Atherton–Sablik model of the magnetoelastic Villari effect. *Arch. Metall. Mater.*, 61, 607–612.

[21] Siemko, A., Lachowicz, H.K. (1990). On the origin of stress-dependent saturation magnetostriction in metallic glasses. *J. Magn. Magn. Mater.*, 89, 21–25.

[22] Szewczyk, R. (2016). Stress-induced anisotropy and stress dependence of saturation magnetostriction in the Jiles–Atherton–Sablik model of the magnetoelastic Villari effect. *Arch. Metall. Mater.*, 61(2), 607–612.

[23] Dubov, A.A., Dubov, A.A., Kolokolnikov, S.M. (2012). *Metal Magnetic Memory method and control devices*. Moscow: Spectrum.

[24] Piotrowski, L., Augustyniak, B., Chmielewski M., Hristoforou, E.V., Kosmas, K. (2010). Evaluation of Barkhausen Noise and Magnetoacoustic Emission Signals Properties for Plastically Deformed Armco Iron. *IEEE Trans. Magn.*, 46(2), 239–242.

[25] Fiorillo, F., Küpferling M., Appin, C. (2018). Magnetic Hysteresis and Barkausen Noise in Plastically Deformed Steel. *Metals*, 8, 15.

[26] JCGM 100:2008. *Evaluation of measurement data — Guide to the expression of uncertainty in measurement*.

[27] Dietrich, E., Schultze, A. (2011). *Measurement Process Qualification: Gauge acceptance and measurement uncertainty according to current standards*. München: Hanser.

[28] Rucki, M., Barisic, B. (2009). Response Time of Air Gauges with Different Volumes of the Measuring Chambers. *Metrol. Meas. Syst.*, 16(2), 289–298.

[29] Joubert, J.W., Meintjes, S. (2015). Repeatability & reproducibility: Implications of using GPS data for freight activity chains. *Transportation Research Part B: Methodological*, 76, 81–92.

[30] Cepova, L., Kovacikova, A., Cep, R., Klaput, P., Mizer, O. (2018). Measurement System Analyses – Gauge Repeatability and Reproducibility Methods. *Meas. Sci. Rev.*, 18(1), 20–27.